Exciton Equilibration Induced by Phonons: Theory and Application to PS II Reaction Centers

Jan A. Leegwater

Department of Physics and Astronomy, Vrije Universiteit Amsterdam, De Boelelaan 1081, 1081 HV-NL Amsterdam, The Netherlands

James R. Durrant and David R. Klug*

Molecular Dynamics Group, Departments of Biochemistry and Chemistry, Imperial College of Science Technology and Medicine, London SW7 2AY, England

Received: October 29, 1996; In Final Form: February 6, 1997[⊗]

In this paper we compare calculations of the rates of excitation energy transfer within reaction center of photosystem II, with transient absorption measurements of the same dynamics. The theory that we apply is based on the assumption that exciton−phonon interaction is fairly weak. In this way we can study the effect of exciton coherence as well as the relaxation toward thermal equilibrium of an excitonically coupled system. The theory correctly predicts the experimentally observed differences in rates for transfer between two degenerate states in the vicinity of 680 nm and transfer between red and blue electronic states.

I. Introduction

In photosynthetic systems, excitation energy is transported between pigments of the antenna to allow the energy to reach the reaction centers. The question whether this transport is coherent or incoherent has attracted a great deal of attention for many years. In spite of this activity, the discussion is in no way close to a consensus. We believe that this is due to the specific values of the parameters that characterize photosynthetic systems. We can identify a number of energies, the relative magnitudes of which determine which approximation is appropriate. These energies are the (exciton) interaction energy J, the homogeneous linewidth γ_0, the temperature T, and the inhomogeneous broadening Δ. The values of some of these parameters are not well established, and those estimates that exist are only accurate within a factor of 2. What is clear is that for photosynthetic complexes all four parameters mentioned are of comparable magnitude. Thus we are in the middle ground for all possible perturbation expansions, and simplified treatments must be evaluated with great care. In the Förster picture, the interaction between pigments is assumed to be small, so that the interaction energy J can be used as a perturbation parameter. In a previous study[1] we have assumed that the temperature is very high, so that again a substantial simplification results. In this paper we use the homogeneous linewidth γ_0 as a perturbation parameter for our theoretical expressions. In this way can we study the effect of exciton coherence as well as the relaxation toward thermal equilibrium. While the assumption of slow homogeneous dephasing may appear to be restrictive, still very reasonable results are obtained for the excited state dynamics.

We apply this theory to exciton equilibration in the isolated reaction center (RC) of photosystem II (PS II). PS II is responsible for water splitting in higher plants. The reaction center at the heart of PS II generates a charge-separated state, the energy of which generates sufficient oxidizing power to remove four electrons from two water molecules during four cycles of the RC. There are a number of published studies of the dynamics and thermodynamics of energy and electron transfer in PS II RCs (for a review see refs 2,3), yet the mechanisms that underlie the observed kinetics are still obscure.

PS II RCs are different from the RCs of purple bacteria such as *Rhodobacter sphaeroides* and *Rhodopseudomonas viridis* in a number of important ways. The issues that concern us here are those that are relevant to excitation energy transfer in these particles. In purple bacterial (PB) RCs the energy transfer is largely unidirectional and toward the lowest exciton state of the special pair.[4] In PS II however, excitation of the reaction center pigments produces a rapid equilibration of excitation energy which is largely complete within 1 ps.[5,6] The exact nature of the equilibrium is both awkward to measure experimentally and problematic to calculate theoretically, but the equilibrium constants must be low, as the energy gaps between the excited electronic states in the PS II RC are only on the order of k_BT at room temperature. The presence of shallow equilibria is supported by femtosecond transient absorption measurements[5,6] and time-resolved emission measurements.[7] We have suggested that one consequence of the small energy gaps in the PS II reaction center is that dipole−dipole coupling leads to the formation of a number of relatively delocalized exciton states.[8] This is known as the multimer model of the PS II reaction center. This is in contrast to the situation in purple bacteria, where dipole-driven delocalization is apparently dominated by the bacteriochlorophyll special pair.

Several groups have published models of the PS II reaction center in which the primary donor electron donor, P680, is modeled as weakly coupled dimer of chlorophylls.[9−11] The multimer model differs from these models in that dipole−dipole coupling is included between all of the central reaction center chlorins (four chlorophylls and two pheophytins) and inhomogeneous broadening of the optical transitions is included in the calculation of the exciton states.[8] A key element of this model is that it is relatively insensitive to the detailed structural arrangement of the chlorins. The multimer model made a number of predictions concerning the static optical properties of the PS II reaction center, including the presence of two degenerate exciton states at 680−684 nm,[8,12] which have high average oscillator strength and whose transition dipoles are nearly orthogonal. We have recently shown that these predic-

[⊗] Abstract published in *Advance ACS Abstracts,* August 15, 1997.

S1089-5647(96)03405-0 CCC: $14.00

tions are in good agreement with experiment.[6] In this paper we examine whether experimental observations of the exciton dynamics within the PS II multimer are also consistent with the predictions of this model.

While these successes are noted, at the same time a number of significant questions remained unanswered. In particular, questions pertaining to the spectral kinetics have not been addressed. In this paper we derive expressions for the energy transfer dynamics of the exciton states. A significant innovation over previously developed theories[1] is that the theory presented here is valid for arbitrary temperatures so that we can study the formation of a thermal equilibrium of exciton states. The transport mechanism described here is a generalization of the Förster transfer mechanism,[13] as it holds irrespective of the strength of the dipole−dipole coupling relative to the intensity of line-broadening mechanisms,[1] and is consequently valid for calculating the rates of excitation energy transfer between exciton states. Below we detail the description of the exciton dynamics. However, some statements can be made without a detailed calculation. It is clear that the density matrix that describes thermal equilibrium $\rho = \exp(-H_0/k_BT)$ does not change in time. Hence, the decay matrix $\hat{\Gamma}$ (see eq 5) acting on this state must give zero, while other states relax toward the equilibrium state. So $\hat{\Gamma}$ necessarily depends on the temperature and also on the Hamiltonian of the system. Moreover, in general it will not be a site-local function, as the various exciton states are in general delocalized. These simple observations already make clear that any exciton theory at finite temperature is necessarily nontrivial.

II. Theory

The Hamiltonian for a system of coupled electronic states in the absence of phonons is

$$H_0 = \sum_i \hbar\omega_i |i\rangle\langle i| + \sum_{i<j} J_{ij}(|i\rangle\langle j| + |j\rangle\langle i|) \qquad (1)$$

where $|i\rangle$ and $|j\rangle$ denote electronic states in which molecule i (or j) is excited. The first term is the energy of the states, while the second represents the coupling between states. In the following we will use the index k to indicate an eigenstate of H_0 (exciton state) with wave function $|\psi_k\rangle$. This exciton state is a linear combination of states $|i\rangle$. Inhomogeneous broadening is taken into account by drawing the isolated molecule transition frequencies ω_i randomly from a certain distribution. The experimental observables are then found from a Monte Cralo simulation.

We now assume that there is also phonon-induced homogeneous broadening. For simplicity we will assume that each molecule has its own heat bath, which is a good approximation when there is no strong phonon-mediated interaction between molecules. In PS II it is known that there is no strongly coupled "marker" mode.[14] Therefore in PSII it appears to be a valid approximation, in contrast to bacterial reaction centers.[15] We have not included the effect of intermolecular distance variations caused by phonons. Although this does affect the dipole coupling, and therefore the electronic Hamiltonian, we expect that this dependence will be much smaller than the diagonal exciton−phonon coupling simply because the energies involved differ by almost 2 orders of magnitude due to the relatively large distances between the molecules. The phonons cause a time dependent shift of the isolated molecule transition frequency; however, they do not give rise to a decrease of the number of excited molecules. This is modeled by an exciton−phonon interaction term

$$V = \sum_{i,q_i} C_{i,q_i} |i\rangle\langle i|(B^\dagger_{i,q_i} + B_{i,q_i}) \qquad (2)$$

Here $B^\dagger$ and B are creation and annihilation operators for the phonons. $C_{i,q}$ is a coefficient coupling a particular electronic state to a particular phonon. Throughout the article we use q_i to indicate a phonon index associated with the molecular state $|i\rangle$. The phonon Hamiltonian is

$$H_{\mathrm{ph}} = \sum_{q_i} \Omega_{q_i} B^\dagger_{i,q_i} B_{i,q_i} \qquad (3)$$

where Ω_q is the phonon frequency. Note that the interaction operator V conserves the number of excited molecules as it commutes with the operator $\sum_i |i\rangle\langle i|$. Hence the phonons give rise to T_2^* (pure dephasing) processes. Irreversible decay, which is commonly denoted as a T_1 process (population loss), is not taken into account in the theory described here.

Equation 2 can be made plausible as follows. The probability of a phonon appearing at a molecule depends on the expectation value of the operators $B^\dagger$ and B. The phonon causes a change in the isolated molecule transition frequency with an amount proportional to $C_{i,q}$. In the end the phonons give rise to loss of phase coherence. To describe this properly, we must use the reduced density matrix $\rho^{(s)}(t)$. The reduced density matrix is the average of the state $|\psi,q_i\rangle$ over the phonon degrees of freedom:

$$\rho^{(s)}(t) = \mathrm{Tr}_{\{q_i\}} |\psi,q_i\rangle\langle\psi,q_i| \qquad (4)$$

Here ψ refers to the electronic part of the total wave function, and q_i to the phonon part. There are two classes of matrix elements in the reduced density matrix. The diagonal elements $\rho^{(s)}_{i,i}$ are the probabilities of finding molecule i in the excited state. The off-diagonal elements $\rho^{(s)}_{i\neq j}$ describe the phase coherence between molecules i and j. The phase coherence between molecules i and j decays when a phonon is absorbed or emitted by molecule i since then the transition frequency is changed, and as a result, the phase is changed by some random amount.

For a general exciton−phonon interaction Hamiltonian V no further progress can be made. However, if we assume that V is smaller than $J_{i,j}$, we can use a perturbation expansion to arrive at kinetic equations. After taking the average over the phonon degrees of freedom, the time evolution of the density matrix is given by[16−21]

$$(\mathrm{d}/\mathrm{d}t)\rho^{(s)}(t) = -\mathrm{i}H_0\rho^{(s)}(t) + \mathrm{i}\rho^{(s)}(t)H_0 - \hat{\Gamma}\rho^{(s)}(t) \qquad (5)$$

The formal expression for the decay matrix $\hat{\Gamma}$ is

$$\hat{\Gamma} = \int_0^\infty \mathrm{d}t \langle\langle \hat{V}(t)\, \hat{V}(0)\rangle\rangle_{\mathrm{ph}} \qquad (6)$$

where the double sharp brackets denote the thermal average over the phonon degrees of freedom and

$$\hat{V}\rho^{(s)} = [V,\rho^{(s)}] \qquad (7)$$

We have

$$V(t) = \exp[\mathrm{i}(H_0 + H_{\mathrm{ph}})t]V\exp[-\mathrm{i}(H_0 + H_{\mathrm{ph}})t] \qquad (8)$$

Notice that $V(t)$ is not a site-local operator due to the (coherent) exciton dynamics in between time 0 and time t.

III. Explicit Expression for the Relaxation Matrix

We are interested in the calculation of the energy transfer rates from one exciton state k_1 of H_0 to another state k. The total evolution equation for the density matrix elements $\rho^{(s)}_{k,k'}$ is given by

$$(\mathrm{d}/\mathrm{d}t)\rho^{(s)}_{k,k'}(t) = -\mathrm{i}(\omega_k - \omega_{k'})\,\rho^{(s)}_{k,k'}(t) - \sum_{k_1,k_1'}\Gamma_{k,k';k_1,k_1'}\rho^{(s)}_{k_1,k_1'}(t) \quad (9)$$

The expression for the decay matrix $\hat{\Gamma}$, eq 6, has four terms when the commutators of $\hat{V}$ are expanded. We will detail one of these four contributions here, as the others can be treated in a similar manner. The time dependence of the operator V is found using eqs 2 and 8 as

$$V(t) = \sum_{i,q_i} C_{i,q_i}\exp(\mathrm{i}H_0t)|i\rangle\langle i|\exp(-\mathrm{i}H_0t)\times (B^\dagger_{i,q_i}\mathrm{e}^{-\mathrm{i}\Omega_{q_i}t} + B_{i,q_i}\mathrm{e}^{-\mathrm{i}\Omega_{q_i}t}) \quad (10)$$

One of the contributions of eq 6, acting on a matrix element $\rho^{(s)}_{k_1,k'_1} = |\psi_{k_1}\rangle\langle\psi_{k'_1}|$, is

$$\Gamma^{(1)}|\psi_{k_1}\rangle\langle\psi_{k_1'}| = \int_0^\infty \mathrm{d}t\langle\langle V(t)|\psi_{k_1}\rangle\langle\psi_{k_1'}|V(0)\rangle\rangle_{\mathrm{ph}} = \sum_{i,q,q'_i}\int_0^\infty \mathrm{d}t\langle\langle C_{i,q_i'}(B^\dagger_{i,q_i}\mathrm{e}^{-\mathrm{i}\Omega_{qi}'t} + B_{i,q_i'}\mathrm{e}^{\mathrm{i}\Omega_{qi}'t})\times C_{i,q_i}(B^\dagger_{i,q_i} + B_{i,q_i})\exp(\mathrm{i}H_0t)|i\rangle\langle i|\exp(-\mathrm{i}H_0t)|\psi_{k_1}\rangle\times\langle\psi_{k_1'}|i\rangle\langle i|\rangle\rangle_{\mathrm{ph}} \quad (11)$$

q This expression is complicated because of the presence of the evolution operators $\exp(\pm\mathrm{i}H_0t)$. When we consider $\Gamma_{k,k';k_1k_1'}$, a substantial simplification results. Then all states involved are eigenstates of H_0 so that the time evolution $\exp(\pm\mathrm{i}H_0t)$ is a simple exponential factor. Moreover, in this case the thermal average over the phonon degrees of freedom can be performed. We have $\langle B^\dagger B^\dagger\rangle = \langle BB\rangle = 0$, $\langle B^\dagger B\rangle = n_{\mathrm{th}}$, and $\langle BB^\dagger\rangle = 1 + n_{\mathrm{th}}$, where the thermal number of phonons is

$$n_{\mathrm{th}}(\omega) = [\exp(\hbar\omega/k_{\mathrm{B}}T) - 1]^{-1} \quad (12)$$

Using these results we obtain

$$\Gamma^{(1)}_{k,k';k_1,k_1'} = \sum_{i,q_i}|C_{i,q_i}|^2\times\int_0^\infty \mathrm{d}t[\mathrm{e}^{-\mathrm{i}\Omega_{q_i}t}n_{\mathrm{th}}(\Omega_{q_i}) + \mathrm{e}^{\mathrm{i}\Omega_{q_i}t}[1 + n_{\mathrm{th}}(\Omega_{q_i})]]\times\exp(\mathrm{i}\omega_k t)\langle\psi_k|i\rangle\langle i|\exp(-\mathrm{i}\omega_{k_1}t)|\psi_{k_1}\rangle\times\langle\psi_{k_1'}|i\rangle\langle i|\psi_{k'}\rangle = \sum_i\gamma_i(\omega_{k_1} - \omega_k)\langle\psi_k|i\rangle\langle i|\psi_{k_1}\rangle\langle\psi_{k_1'}|i\rangle\langle i|\psi_{k'}\rangle \quad (13)$$

where the time integral can be replaced by a delta function:

$$\gamma_i(\omega_{k_1} - \omega_k) = \sum_{q_i}|C_{i,q_i}|^2\{n_{\mathrm{th}}(\omega_k - \omega_{k_1})\delta(-\Omega_{q_i} + \omega_k - \omega_{k_1}) + [1 + n_{\mathrm{th}}(\omega_{k_1} - \omega_k)]\delta(\Omega_{q_i} + \omega_k - \omega_{k_1})\} \quad (14)$$

Only one of the two delta functions will be nonzero as $\Omega_{q_i} > 0$. Because of this, $\gamma(\omega)$ satisfies the thermal equilibrium condition

$$\gamma(-\omega) = \exp(-\hbar\omega/k_{\mathrm{B}}T)\gamma(\omega) \quad (15)$$

It is in the end through this relation on $\gamma(\omega)$ that the time evolution satisfies the detailed balance condition, eq 12. The reader may wonder where this sensitivity for the temperature of the environment has been introduced. The answer is that it is already present in the formal expression for the relaxation matrix $\hat{\Gamma}$, eq 6. This expression is more subtle than would appear on first sight. The consequence of this subtlety becomes explicit in eq 14, where a distinction between positive and negative frequencies is made. For downhill energy transfer, $\omega_{k_1} > \omega_k$, and the contribution proportional to $(1 + n_{\mathrm{th}})$ in eq 14 is selected. For uphill transfer we find only the factor n_{th}. Note that $n_{\mathrm{th}}(\omega)/[1 + n_{\mathrm{th}}(\omega)] = \exp(-\hbar\omega/k_{\mathrm{B}}T)$. The difference between positive and negative frequencies can in the end be traced back to the time ordering of the superoperators $\hat{V}$ in eq 6. The Boltzmann statistics comes out because of the difference between absorption and emission of phonons; only for downhill energy transfer is there a contribution from spontaneous emission of phonons.

We will assume that all environments are identical so that γ_i does not depend on the molecule index i. When the other contributions to $\hat{\Gamma}$ are added, we finally find

$$\Gamma_{k,k';k_1k_1'} = \delta_{k',k_1'}\sum_{K,i}\gamma(\omega_k - \omega_K)\langle\psi_k|i\rangle|\langle i|\psi_K\rangle|^2\langle i|\psi_{k_1}\rangle + \delta_{k,k_1}\sum_{K,i}\gamma(\omega_{k'} - \omega_K)\langle i|\psi_{k'}\rangle|\langle i|\psi_K\rangle|^2\langle\psi_{k_1'}|i\rangle - [\gamma(\omega_{k_1} - \omega_k) + \gamma(\omega_{k_1'} - \omega_{k'})]\times\sum_i\langle\psi_k|i\rangle\langle i|\psi_{k_1}\rangle\langle\psi_{k_1'}|i\rangle\langle i|\psi_{k'}\rangle \quad (16)$$

The spectral density $\gamma(\omega)$ describes the frequency dependent coupling of the complex to its environment. The exact nature of γ is system dependent, but we can make an educated guess regarding its properties. The derivation, which is based on harmonic oscillators, not only gives the relaxation matrix Γ but also predicts the complete temperature dependence of Γ. We denote the zero temperature limit of $\gamma(\omega)$ by $\gamma_0(\omega)$. Then

$$\gamma(\omega) = \begin{cases}[1 + n_{\mathrm{th}}(\omega)]\gamma_0(\omega) & (\omega > 0)\\ n_{\mathrm{th}}(-\omega)\,\gamma_0(-\omega) & (\omega < 0)\end{cases} \quad (17)$$

For low temperatures this may be a realistic approximation, but its validity at room temperature is questionable. PS II is not made of harmonic oscillators, and it even goes through a phase transition between 200 and 250 K, so a straightforward extrapolation from zero temperature is impossible. All calculations presented so far in this section are for harmonic oscillators; the expression for Γ is generally valid in this case, provided that γ is small. The results of this section can be used at room temperature by introducing a temperature dependent γ_0, or by simply making an assumption for $\gamma(\omega)$. The only physical constraint on the function γ is that it is compatible with thermal equilibrium eq 15. In the following we will assume that

$$\gamma(\omega) = \frac{2\gamma_0}{1 + \exp(-\hbar\omega/k_{\mathrm{B}}T)} \quad (18)$$

This $\gamma(\omega)$ describes a coupling that, apart from the thermal effect just mentioned, is independent of frequency. The infinite temperature limit of eq 18 is frequency independent and corresponds to an environment correlation time of zero, which is usually denoted the fast modulation limit. Equation 18 can be considered as the extension of an exponential decay to finite temperatures. We expect that this is a reasonable assumption for the >100 fs time scales considered here. A detailed discussion of possible alternatives for eq 18 is beyond the scope of this paper.

TABLE 1: Exciton Interaction Energies H_0 in cm^{-1} for the Model of the PS II Reaction Center Shown in Figure 1: This Hamiltonian Is Identical to the One Used in Ref 8[a]

Ph1	Ch1	Ch2	Ch3	Ch4	Ph2
$\omega_0 + d_1$	86.3	17.3	−1.2	−5.7	2.7
	$\omega_0 + d_2$	−101	−42.7	15.8	−5.5
		$\omega_0 + d_3$	120	−37.9	−1.7
			$\omega_0 + d_4$	−90.2	17.2
				$\omega_0 + d_5$	82.3
					$\omega_0 + d_6$

[a] The diagonal elements are the monomer transition energies, where $\omega_0 = 14\,860$ cm^{-1}.

In the following we will only study the populations, which are the diagonal elements ($k = k'$) of $\rho^{(s)}$. The dynamics is described by the master equation

$$(\mathrm{d}/\mathrm{d}t)\rho^{(s)}_{k,k}(t) = -\sum_{k_1}\Gamma_{k,k;k_1k_1}\rho^{(s)}_{k_1,k_1}(t) \tag{19}$$

with the population transfer rates

$$\Gamma_{k,k;k_1k_1} = 2\delta_{k,k_1}\sum_{i,K}\gamma(\omega_{k_1} - \omega_K)|\langle i|\psi_K\rangle|^2|\langle i|\psi_{k_1}\rangle|^2 - 2\sum_i\gamma(\omega_{k_1} - \omega_k)|\langle i|\psi_k\rangle|^2|\langle i|\psi_{k_1}\rangle|^2 \tag{20}$$

Because of eq 15, we have

$$\Gamma_{k,k;k_1k_1} = \exp\left(\frac{\hbar\omega_{k_1} - \hbar\omega_k}{k_\mathrm{B}T}\right)\Gamma_{k_1,k_1;k,k} \tag{21}$$

which is the usual detailed balance condition.[21] The set of time evolution equations 9 and 16 is more general and may be used to describe the effect of exciton coherence. To briefly summarize where we stand now, in order to calculate the relaxation rates, all that is needed is the exciton Hamiltinian H_0 and a reasonable approximation for $\gamma(\omega)$.

IV. Simulation of Exciton Equilibration in Photosystem II

In this section we employ eq 19 to calculate the dynamics of exciton equilibration in the PS II reaction center. These exciton states are eigenstates of the Hamiltonian H_0 defined in eq 1. We have previously proposed a Hamiltonian for the PS II reaction center.[8] We use the same Hamiltonian here (Table 1). The Hamiltonian was calculated employing the point dipole approximation for the interaction strengths J_{ij}, and assuming a PS II reaction center structure corresponding to that of the purple bacterium *R. viridis*, but with a reduced coupling of the special pair chlorophylls. The model does not include peripheral reaction center chlorophylls, as it has been shown that these are only weakly coupled to the core reaction center pigments.[22]

Our previous calculations took into account all the dipole−dipole couplings between core reaction center chlorins, as well as static inhomogeneous broadening,

$$\hbar\omega_i = \hbar\omega_0 + d_i \tag{22}$$

where the inhomogeneous shifts d_i (energy level disorder) were taken to exhibit a Gaussian probability distribution with width Δ_{inh}. Our calculations employing this model indicated that the core PS II reaction center chlorins should be considered a multimer of excitonically coupled pigments, with each exciton state delocalized over approximately three pigments. In this calculation the delocalization was limited only by the inhomogeneous disorder, as no phonons were taken into account. As was shown in ref 1, the validity of this approach for antenna systems is limited, but inhomogeneous broadening may well be the dominant factor in PS II RCs. Crucially, as the optical properties of this multimer are aggregate properties of several pigments, the model was relatively insensitive to the details of the structure employed in the calculation of H_0. We have demonstrated that this model exhibits a good agreement with a wide range of experimental observations of the static optical properties of the PS II reaction center. In particular, the model predicted the presence of two approximately degenerate optical transitions of the multimer between 680 and 684 nm with near orthogonal transition dipoles. The predicted optical properties of these transitions (orientation and oscillator strength) were subsequently verified experimentally, with a quantitative agreement being found between theoretical predictions and experiment.[6]

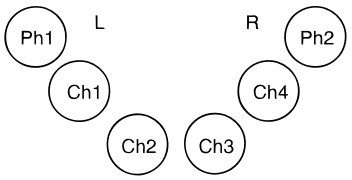

Figure 1. Schematic representation of the assumed locations of the pigments of PS II as employed in ref 8. Ph denotes Pheophytin, and Ch denotes Chlorophyll. The structure is based on the *Rh. viridis* structure with the separation of the central dimer increased by 0.28 nm along their connecting axis.

We have previously resolved transient absorption kinetics[6] which we have assigned to population dynamics associated with these two 680−684 nm transitions. Two examples of such data are reproduced in Figure 2a,c. These data are the isotropic transient absorption signal (Figure 2a), and the corresponding anisotropy (Figure 2c), observed at a probe wavelength of 683 nm following photoselective excitation of isolated PS II reaction centers. We have previously shown that these excitation conditions result in the selective excitation of the two 680−684 nm transitions. We have assigned the isotropic signal at 683 nm to bleach/stimulated emission caused by population of these states, with the ∼100 fs recovery of the initial signal being attributed to population transfer to higher energy 665−676 nm exciton states.[5,6] The anisotropy at 683 nm exhibits a ∼400 fs decay, which we have assigned to transfer of population between the two orthogonal 680−684 nm transitions.[6]

Figure 2b,d shows the results of numerical simulations of these experimental data. These simulations follow directly from our previous calculations of the static optical properties of the PS II multimer and employing eq 18 for the form of the spectral density function $\gamma(\omega)$. Following calculation of the transfer rates from eq 19, determination of the population dynamics can be readily determined by the inclusion of appropriate initial excitation conditions. As previously, we include static energy level disorder in the calculations; determination of the ensemble-averaged dynamics is achieved by averaging of the population dynamics calculated for 2000 different realizations of the energy level shifts ($\Delta_{\mathrm{inh}} = 210$ cm^{-1} as previously). Full details of these simulations are given in the Appendix.

It is apparent from Figure 2 that we obtain an excellent agreement between our experimental and simulation results. It should be emphasized that these simulations were conducted without the use of any variable parameters. The simulations employed the same Hamiltonian we have previously used to model the static optical properties of the PS II reaction center.[6,8] The only additional input required was the determination of an appropriate spectral density function for the phonons of the system eq 18, and the value of γ_0. A value of 200 cm^{-1} was taken for γ_0, as this seems to be the most reliable estimate for the homogeneous dephasing rate.[23] The simulations show agreement with the experimental data not only in the final

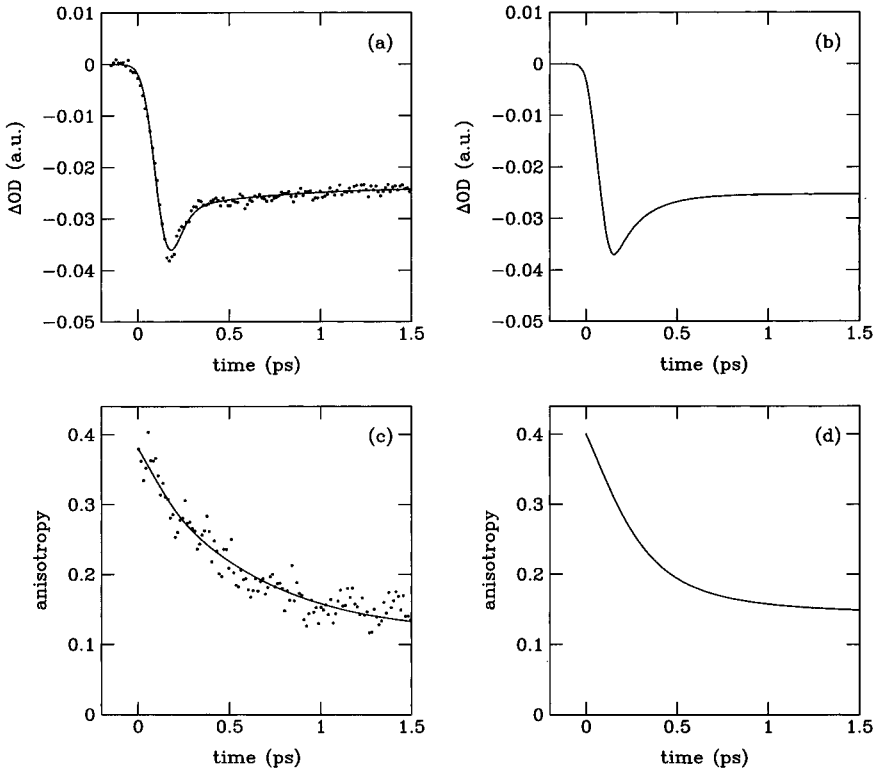

Figure 2. Comparison of the results of experimental studies (a and c) of isolated PS II reaction centers at 10 °C with numerical simulations (b and d). Experimental transient absorption data are taken from ref 6; the data were collected at a probe wavelength of 683 nm following 694 nm excitation. Parts a and c show the isotropic signal and the transient anisotropy, respectively. The smooth lines are the results of multiexponential analyses of these data (see ref 6 for details). Parts b and d show the simulated isotropic and anisotropy signals, respectively, these were calculated using eq 19 and employed a reaction center Hamiltonian taken from ref 8. Full details of these simulations are given in the Appendix.

anisotropy value and the proportion of the initial isotropic signal decaying on this time scale but also in their kinetics. The simulated isotropic data exhibit a recovery with a time constant 3 times faster than the corresponding decay of the anisotropy signal, in good agreement with the factor of 4 obtained experimentally.[24]

It should be emphasized that these simulations include a number of approximations and simplifications. For example, contributions to the experimental data from excited state absorption (and in particular the one-exciton to two-exciton transition) are neglected.[25] However, even at this level of simplification, the simulations are able to reproduce reasonably well the time constant and magnitude of 100 fs recovery of the isotropic bleach/stimulated emission observed experimentally and the time constant and magnitude of the 400 fs anisotropy decay. These simulations confirm our previous conjecture that the slower decay of the anisotropy relative to the isotropic signal results from the partitioning of the two 680 nm transitions over, on average, opposite arms of the reaction center. The wave function overlap between these ~680 nm transitions is therefore small, resulting in a slower rate of population transfer between them.

Acknowledgment. The research of J.A.L. has been made possible by a fellowship of the Royal Netherlands Academy of Arts and Sciences (KNAW). We also thank The Royal Society, BBSRC, EU, and RITE for financial support.

Appendix: Numerical Simulation of the Experimental Data

The transition energies (ω_k) and dipoles ($\vec{\mu}_k$) of the PS II reaction center exciton states were calculated by diagonalization of eq 1, as detailed in reference.[8] The population transfer rates were then calculated from eq 19. The population of each exciton state as a function of time can then be readily calculated by the inclusion of appropriate initial starting conditions. The experimental data employed excitation pulses that selectively excite the two lowest energy exciton transitions, and a probe wavelength that monitored the bleach/stimulated emission from these states.[6] Numerical simulations were therefore carried out for initial population of either of these transitions and neglected excited state absorption.[25] For each excitation condition, numerical simulations were conducted for parallel and perpendicular orientations of the transient ΔOD signal. An average was obtained of the results for these two excitation conditions, weighted by the oscillator strengths of these transitions. The isotropic and anisotropic signals were then calculated from these simulated data as previously.[6]

As previously, we included inhomogeneous broadening of the monomer transition energies in our calculations. For each calculation, inhomogeneous shifts were selected at random from a Gaussian probability function (fwhm of 210 cm^{-1}), and the resultant isotropic and anisotropy simulations determined. Comparison with the experimental data was conducted after ensemble averaging over 2000 such calculations.

References and Notes

(1) Leegwater J. A. *J. Phys. Chem.* **1996**, *100*, 14403−14409.

(2) van Grondelle, R.; Dekker, J. P.; Gillbro, T.; Sundstrom, V. *Biochim. Biophys. Acta* **1994**, *1087*, 1−65.

(3) Diner, B. A.; Babcock, G. T. In *Oxygenic Photosynthesis: The light reactions*; Yocum, C., Ort, D., Eds.; Kluwer Academic Publishers: Dordrecht, 1996.

(4) Jonas, D. M.; Lang, M. J.; Nagasawa, Y.; Joo, T.; Fleming, G. R. *J. Phys. Chem.* **1996**, *100*, 12660−12673.

(5) Durrant, J. R.; Hastings, G.; Joseph, D. M.; Barber, J.; Porter, G.; Klug, D. R. *Proc. Natl. Acad. Sci. U.S.A.* **1992**, *89*, 11632−11636.

(6) Merry, S. A. P.; Kumazaki, S.; Tachibana, Y.; Joseph, D. M.; Porter, G.; Yoshihara, K.; Barber, J.; Durrant, J. R.; Klug, D. R. *J. Phys Chem.* **1996**, *100*, 10469−10478.

(7) Booth, P. J.; Crystall, B.; Ahmad, I.; Barber, J.; Porter, G.; Klug, D. R. *Biochemistry* **1991**, *30*, 7573−7586.

(8) Durrant, J. R.; Klug, D. R.; Kwa, S. L. S.; Grondelle, R. van; Porter, G.; Dekker, J. P. *Proc. Natl. Acad. Sci. U.S.A.* **1995**, *92*, 4798.

(9) Bosch, M. K.; Proskuryakov, I. L.; Gast, P.; Hoff, A. J. J. *J. Phys. Chem.* **1995**, *99*, 15310−15316.

(10) Mulkidjanian, A. Y.; Cherepanov, D. A.; Haumann, M.; Junge, W. *Biochemistry* **1996**, *35*, 3093−3107.

(11) Svensson, B.; Etchebest, C.; Tuffery, P.; van Kan, P.; Smith, J.; Styring, S. *Biochemistry* **1996**, *35*, 14486−14502.

(12) Groot, M.-L.; Peterman, E. J. G.; Kan, P. J. M. van; Stokkum, I. H. M. van; Grondelle, R. van *Biophys. J.* **1994**, *67*, 318.

(13) Förster, Th. In *Modern Quantum Chemistry*; Sinannoglu, O., Ed.; Academic Press: New York, 1965; p 93.

(14) Chang, H.-C.; Jankowiak, R.; Reddy, N. R. S.; Yocum, C. F.; Picorel, R.; Seibert, M.; Small, G. J. *J. Phys. Chem.* **1994**, *98*, 7725−7735.

(15) Johnson, S. G.; Tang, D.; Jankowiak, R.; Hayes, J. M.; Small, G. J.; Tiede, D. M. *J. Phys. Chem.* **1989**, *93*, 5953−5957.

(16) Kenkre, V. M. In *Exciton Dynamics in Molecular Crystals and Aggregates*; Kenkre, V. M., Reineker, P., Eds.; Springer: Berlin, 1982. See also the article of P. Reineker in this book.

(17) Wannier, G. *Elements of Solid State Theory*; Cambridge: Cambridge, 1959.

(18) Haken, H.; Strobl, G. *Z. Phys.* **1973**, *262*, 135.

(19) Kubo, R. *J. Phys. Soc. Jpn.* **1954**, *9*, 935. Kubo, R.; Toda, M.; Hashitsume, N. *Statistical Physics*; Springer: Berlin, 1985; Vol. 2.

(20) Weiss, U. *Quantum Dissipative Systems*; World Scientific: Singapore, 1993.

(21) Mukamel, S. *Principles of Nonlinear Optical Spectroscopy*; Oxford: New York, 1995.

(22) Rech, T.; Durrant, J. R.; Joseph, D. M.; Barber, J.; Porter, G.; Klug, D. R. *Biochemistry* **1994**, *33*, 14768−14774.

(23) Bradforth, S. E.; Jiminez, R.; Van Mourik, F.; Van Grondelle, R.; Fleming, G. R. *J. Phys. Chem.* **1995**, *99*, 16179.

(24) The simulations do not exhibit monoexponential kinetics, due to the inclusion of inhomogeneous broadening and multiple exciton states in the calculations. However approximate decay times for the simulated data were obtained from crude monoexponential fits to the data, yielding decay time constants of 110 and 300 fs for the isotropic and anisotropy data, respectively.

(25) The experimental difference spectra over this spectral region are dominated by a negative feature resulting from ground state bleach and stimulated emission. Excited state absorption apparent at longer and shorter wavelengths than this feature is relatively weak and structureless.